Dynamic load on a pipe caused by acetylene detonations – experiments and theoretical approaches

Axel Sperber *, Hans-Peter Schildberg and Steven Schlehlein

BASF Aktiengesellschaft, Engineering R&D, D-67056 Ludwigshafen, Germany
Tel.: +49 621 60 56049; Fax: +49 621 60 56934; E-mail: hans-peter.schildberg@basf-ag.de

Received 5 January 1998
Revised 7 January 1999

The load acting on the wall of a pipe by a detonation, which is travelling through, is not yet well characterized. The main reasons are the limited amount of sufficiently accurate pressure time history data and the requirement of considering the dynamics of the system. Laser vibrometry measurements were performed to determine the dynamic response of the pipe wall on a detonation. Different modelling approaches were used to quantify, theoretically, the radial displacements of the pipe wall. There is good agreement between measured and predicted values of vibration frequencies and the propagation velocities of transverse waves. Discrepancies mainly due to wave propagation effects were found in the amplitudes of the radial velocities. They might be overcome by the use of a dynamic load factor or improved modelling methods.

Keywords: Laser vibrometry, acetylene, detonation, pipeline, radial vibrations, measurement, simulation

1. Introduction

Explosions of gases occurring in pipelines may be deflagrative (i.e., the reaction front propagates with a speed much lower than the speed of sound of the gas, whilst the pressure front moves with sonic speed) or detonative (i.e., the reaction front is coupled to a shock wave and propagates with a speed higher than speed of sound), depending on the thermodynamic properties of the gas, the geometry of the pipeline and the initial pressure. Further background details are given in [2,3,7,8].

The shock wave associated with detonations is characterized by a short-time, extremely high pressure pulse (Fig. 1). In case of acetylene detonations, the propagation speed of the reaction front is about 2000 m/s. Typical peak values of the pressure pulses in a long tube are about 30 to 50 times the initial pressure (Fig. 2), typical widths are in the range of 0.03–1.0 milliseconds (full width at half maximum, FWHM).

For safe operation of pipeline transport and handling of acetylene ("detonation proof design"), the stresses caused by those high pressure pulses have to be withstood by the pipe wall. For design purposes, theoretical approaches may be used which have to be backed by experiments. These experiments concern the pressure history, the radial vibrations and the actual dynamic stresses in the pipe wall as well as the material properties of the steel in the case of fast dynamic loading.

The *static approach* (I) for calculating the required thickness of the wall is not adequate here since the short pressure pulse excites the radial vibration modes of the pipe. This implies effects like overshooting, but also attenuation due to the inertia of the mass of the wall and changes of the material properties due to extremely high strain rates. The static approach is only valid in cases of a moderate rates of pressure rise (e.g., deflagrative explosions).

A *dynamic approach* (II) may be achieved by deriving an analytic expression for the fundamental radial vibration mode. This approach assumes that the radial displacements as well as the excitation are symmetric. Wave propagation is not taken into account. Within this model, analytical calculation of strain and stress is possible by a linear-elastic model.

*Corresponding author: Axel Sperber, WINGAS GmbH, P.O. Box 104020, D-34112 Kassel, Germany. Tel.: +49 561 301 1330; E-mail: axel.sperber@wingas.de.

Shock and Vibration 6 (1999) 29–43
ISSN 1070-9622 / $8.00

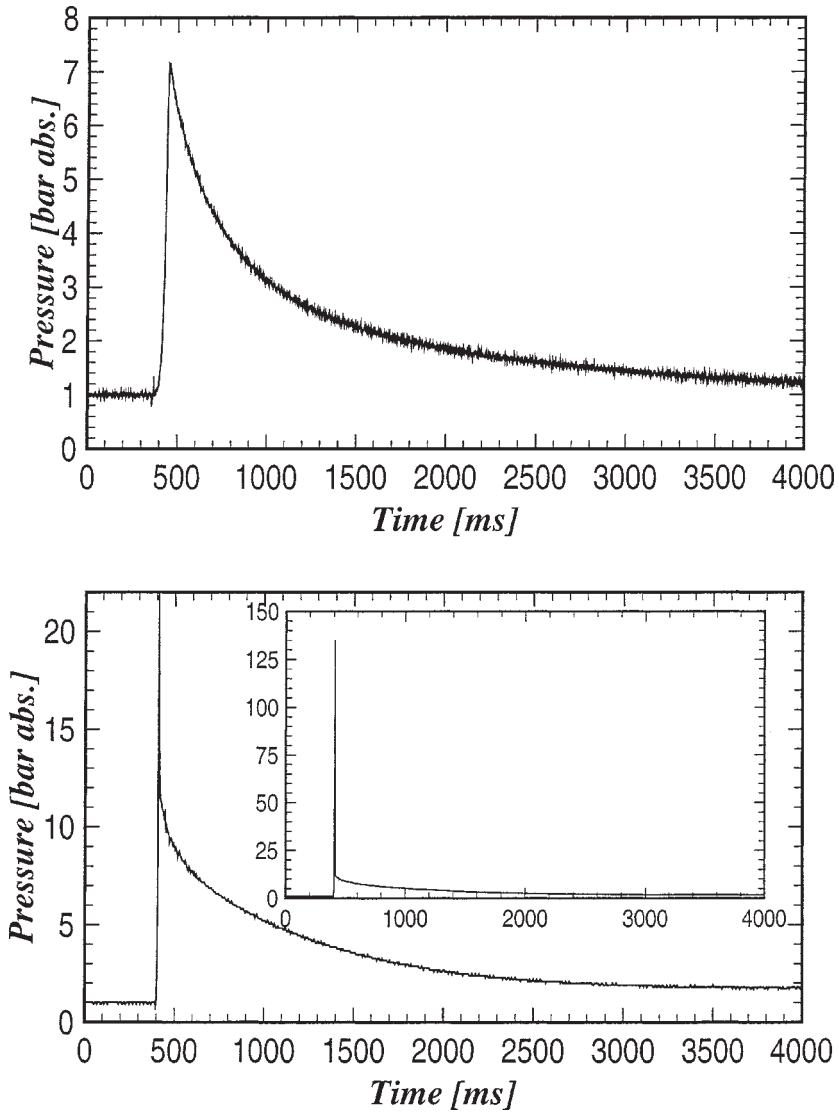

Fig. 1. Differences in the pressure/time trace of a deflagrative (upper diagram) and a detonative explosion (lower diagram). The initial pressure was 1 bar abs in both cases. The maximum rate of pressure rise for deflagrations is typically below 1000 bar m/s (normalized for volume), the maximum explosion pressure is typically 7 to 12 times the initial pressure. Detonative explosions exhibit in the leading edge of the pressure/time trace a very high and short pressure pulse associated with a shock wave which does not appear in deflagrations. The pressure rise of this pulse is faster than can be measured with piezoelectric pressure sensors ($>10^8$ bar/s), the height of the pulse depends on the kind of gas and the geometry of the gas volume (here 135 times the initial pressure was attained, the gas was CH_3-O-NH_2).

An improvement to approach II is done by performing finite element calculations of the vibration modes. Here, as well non-symmetric effects can be included. However, non-linear effects such as plastification are not considered.

A physically more correct and detailed approach is the *wave propagation approach* (III), see [4]. It takes into account the effect of travelling waves through the pipe wall. There is the possibility of resonances if the velocities of the detonation front and the wave speed in the wall are in the same order of magnitude. From a mathematical point of view the pipe has to be treated as a continuous system which does not allow simple analytic expressions for the pipe wall vibrations.

In this study, laser velocimetry measurements of the pipe wall exposed to a detonation are performed in or-

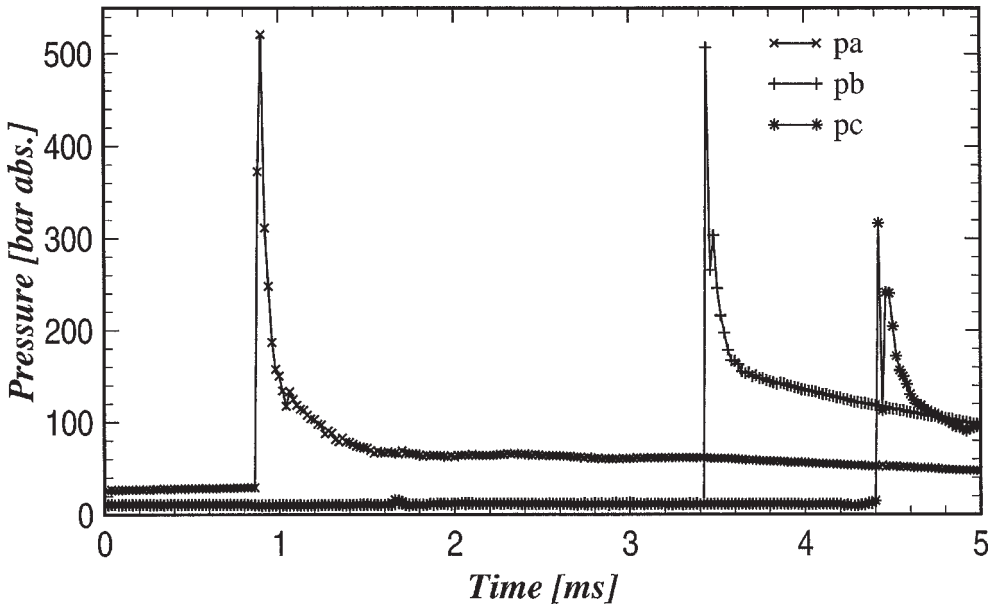

Fig. 2. Pressure/time traces of a detonation propagating through 10 bar acetylene in a $\phi_i = 6$ mm pipe. The pressure sensors p_a, p_b and p_c (type PCB113A03, range 1035 bar, resonance frequency 500 kHz) were mounted in the wall of the tube. p_a was mounted most closely to the point of ignition (500 mm). The distances between the sensors were: p_a to p_b 4410 mm; p_b to p_c 1750 mm. The sampling interval was 20 μs.

der to determine the vibration modes excited by the detonation and to check the measured displacements of the wall from rest position against theoretical predictions. Approach II is predominantly used for modelling. However, approach III is occasionally adopted to explain the results.

Other studies in a similar context are described in [5].

2. Experimental setup

A schematic drawing of the experimental setup is shown in Fig. 3. It basically consists of two straight pipes (inner radius $R_i = 15$ mm, outer radius $R_a = 24$ mm, total length $L = 6$ m, material 1.0305). A pressure sensor was mounted in the lens-like metallic seal between the flanges of both pipes (position 2). The right end of the pipeline was closed by a blind flange (position 4). The flanges are fixed to prohibit movements sideways which may affect the measurement of the radial displacements.

The experimental procedure is as follows: The evacuated pipeline is filled with acetylene up to pressures of about 10, 15 or 20 bar. Then the acetylene is ignited by a melting platinum wire at the left end of the pipeline. At first the decomposition proceeds deflagrative, i.e., the reaction front starts to propagate through the pipe with a speed much lower than the speed of sound whereas the resulting pressure front itself moves with sonic speed (338 m/s for 1 bar abs). With increasing temperature the reaction front is accelerating. The transition from deflagration to detonation occurs within a small distance from the point of ignition (less than 1.5 m for the pressures cited above). The reaction front is now coupled with a shock wave which exhibits a very high pressure amplitude and moves with a constant speed of about 2000 m/s through the pipe. At the closed end, the shock wave is reflected. Hence the pressure acting on the blind flange is twice as high as the pressure acting on the pipe wall.

3. Measurement devices

3.1. Pressure measurement

For the measurement of the pressure time history, which is important for quantifying the source of the excitation of the wall, a piezoelectric transducer PCB 113A03 (range 0–1035 bar, resonance frequency 500 kHz) was used at position 2 of the test rig. It is mounted flush with the inner surface of the pipe wall to avoid disturbances in the measured signal.

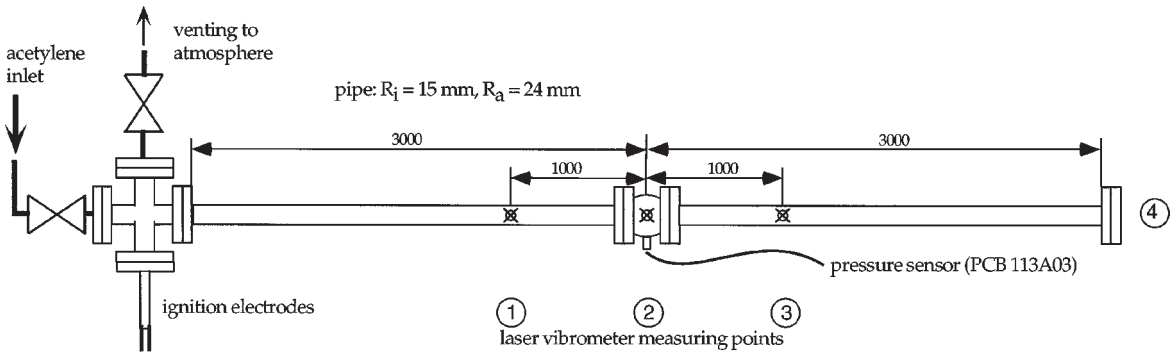

Fig. 3. Experimental setup for measuring the oscillations excited in the wall of a pipe (inner radius $R_i = 15$ mm, outer radius $R_a = 24$ mm, wall thickness 9 mm) by detonations of acetylene at initial pressures up to 20 bar.

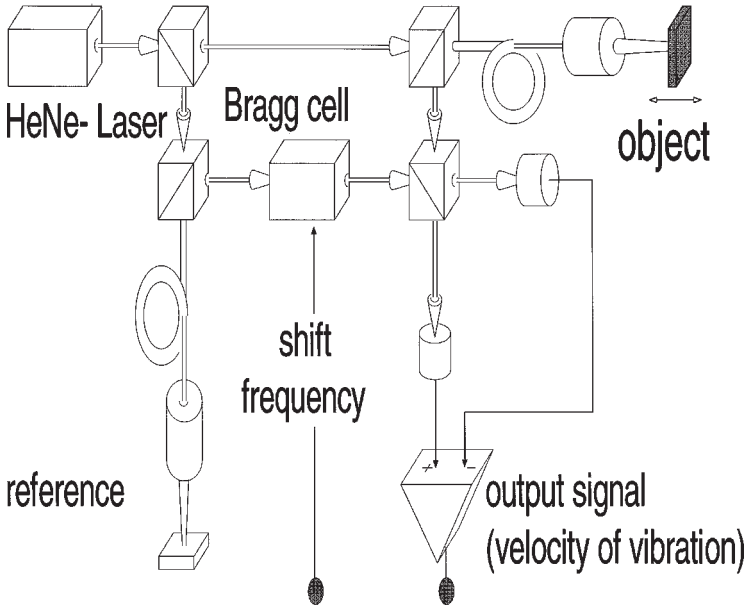

Fig. 4. Fiberoptic laser vibrometer.

3.2. Vibration measurement

For the radial vibrations which determine the dynamic stress in the wall of the pipe, a frequency range of up to 100–150 kHz with very small amplitudes and very high accelerations was to be expected for the pipe under consideration. For this application, piezoelectric accelerometers are not practically suitable. Therefore a fiberoptic two-point laser vibrometer POLYTEC OFV 502 with vibrometer controller OFV 3000 and velocity demodulator OVD 01 was chosen for measuring the radial and axial displacements (schematic Fig. 4). Since the determination of the radial vibration modes without rotational symmetry requires a second channel oriented perpendicular to the first one, an additional laser vibrometer POLYTEC OFV 303 was installed.

3.3. Data acquisition

The pressure and the vibration signals were recorded simultaneously by a PC equipped with a 200 kHz A/D converter board. For antialiasing the charge amplifier of the pressure sensors was equipped with a 100 kHz low-pass filter. As a second recording device operated simultaneously with the PC a RACAL store 7 DS tape recorder was used. The frequency analysis was performed on a 400 kHz real time signal analyzer YOKOGAWA SA2400.

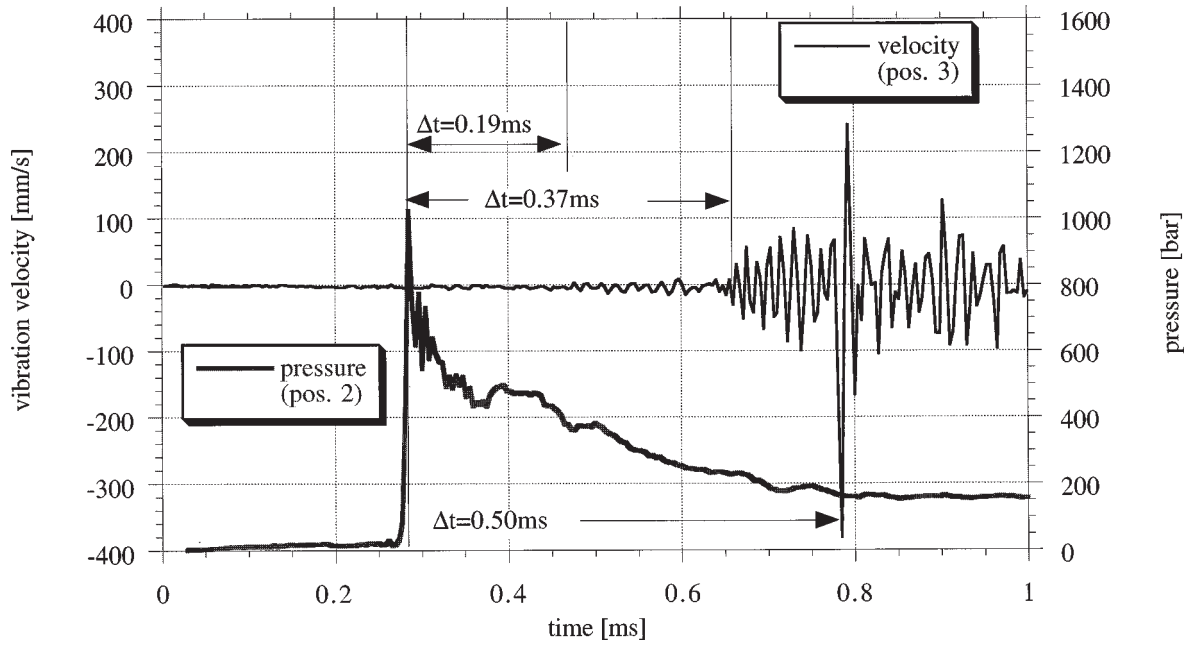

Fig. 5. Time series of pressure and vibration velocity.

To relate the data measured by the pressure transducer to the data recorded by the laser vibrometer with respect to time difference, the difference between the delay times of the indivual devices due to signal processing effects must be known. By recording both signals at the same position (position 2) the difference was found to be negligible (in the order of magnitude of few nanoseconds). For the actual vibration measurements the pressure sensor had to be installed at some distance from the axial position sensed by the laser, because otherwise it would destroy the rotational symmetry of the wall and thus distort the vibration data.

4. Measurement results

In the following sections, the results of a series of 19 experiments with different initial pressures between 11 and 21 bar are described. The pressure was always measured at axial position 2, the vibration velocities of the pipe wall were measured at position 3 in two directions oriented perpendicular to each other (in the following referred to as horizontal and vertical).

4.1. Time delay

Figure 5 gives a typical example of a measured time trace of pressure and radial vibration velocity of the pipe. Since the distance Δx between position 2 (pressure sensor) and position 3 (vibration sensor) is exactly $\Delta x = 1$ m, the vibration signal will appear later than the pressure signal. The time difference Δt between the main peaks of $\Delta t = 0.5$ ms proves the propagation speed v of the shock wave to be $v = \Delta x/\Delta t = 2000$ m/s. It can also be perceived that the pipe wall is beginning to vibrate earlier: small vibrations are starting at $\Delta t = 0.19$ ms, larger vibrations at $\Delta t = 0.37$ ms. To understand these effects, one first has to look at wave propagation. In the pipe wall, longitudinal as well as transverse waves may propagate. The corresponding wave speeds c_L and c_T are determined by material constants and the pipe geometry, as

$$c_\mathrm{L} = \sqrt{\frac{E}{\rho}}, \qquad c_\mathrm{T} = c_\mathrm{L}\sqrt{\frac{R_\mathrm{a} - R_\mathrm{i}}{\sqrt{3}\,\overline{R}(1-\nu^2)}},$$

$$\overline{R} = \frac{R_\mathrm{a} + R_\mathrm{i}}{2}.$$

E is the modulus of elasticity ($E = 2.0 \times 10^{11}$ N/m^2) of the pipe material, ρ is the density ($\rho = 7900$ kg/m^3), $\nu = 0.3$ is the Poisson number. In our case $c_\mathrm{L} = 5030$ m/s and $c_\mathrm{T} = 2720$ m/s, which is higher than the propagation speed of the detonation front. The corresponding transversal wave Mach number is Ma$= v/c_\mathrm{T} = 0.74$. The time delays for the onset of the small vibrations are perfectly explainable if these radial dis-

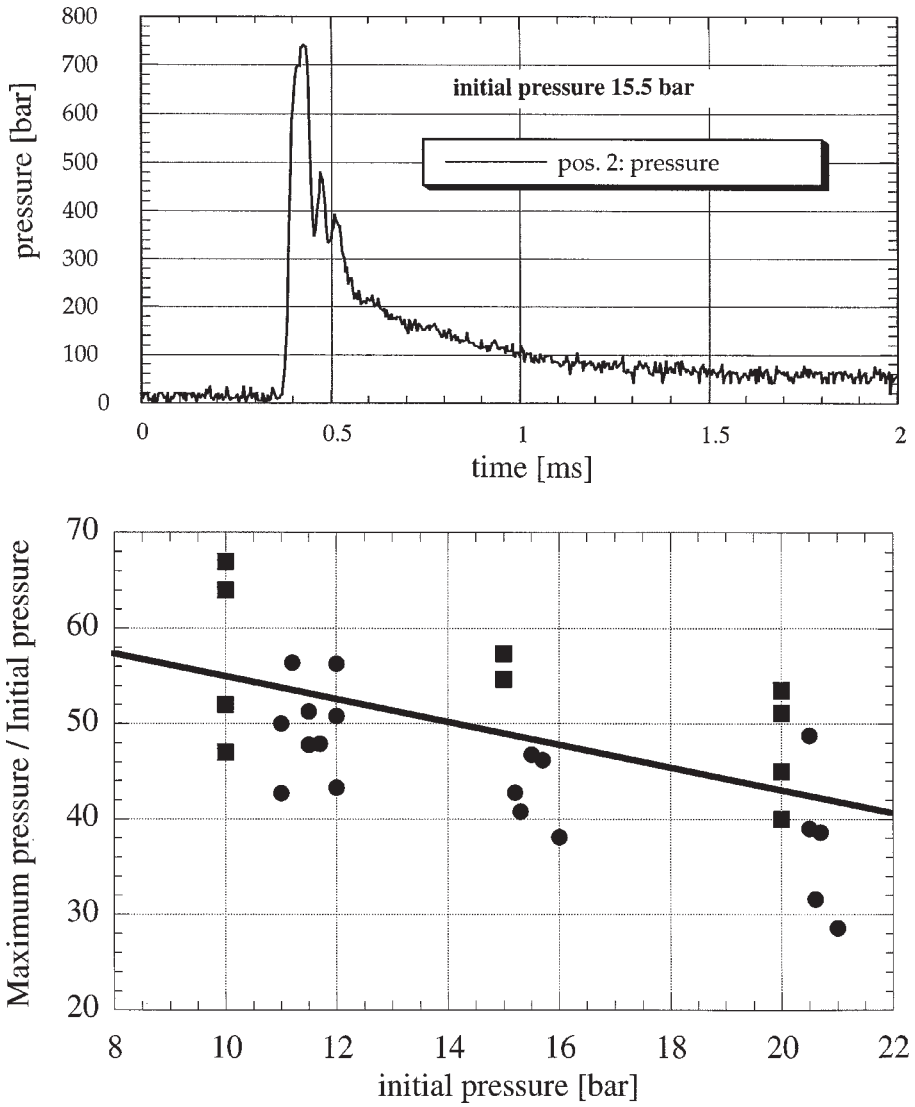

Fig. 6. Top diagram: Pressure–time history of a stable detonation propagating in a $\phi_i = 30$ mm pipe at 15.5 bar initial acetylene pressure. Bottom diagram: Detonation pressure ratios of acetylene as function of the initial acetylene pressure (squares and circles denote data from pipes with $\phi_i = 10$ mm and $\phi_i = 30$ mm, respectively).

placements are associated with a longitudinal wave (although the amplitude of this wave is parallel to the axis of the pipe, there will be small displacements perpendicular to the axis because of the lateral contraction) and a transverse wave which had been excited in the pipe when the detonation front passed the flange, i.e., axial position 2: $\Delta x/0.19$ ms $= 5263$ m/s equals c_L, $\Delta x/0.37$ ms $= 2700$ m/s equals c_T. Apparently the impedance of the flange connection of the two pipes is too high to let pass noticeable amplitudes of the longitudinal and transverse waves, which had been excited in the left 3 m pipe (i.e., the pipe adjacent to the point of ignition), through to the right 3 m pipe. Otherwise one would have to detect some vibrations at position 3 even before the detonation passed position 2.

4.2. Pressure

The upper diagram of Fig. 6 shows an example for the time history of the detonation pressure pulse (here for 15.5 bar initial pressure). For all 19 experiments conducted the FWHM was between 0.1 ms and 0.15 ms. FFT analysis shows typical noisy behaviour. The lower diagram displays the pressure ratio as func-

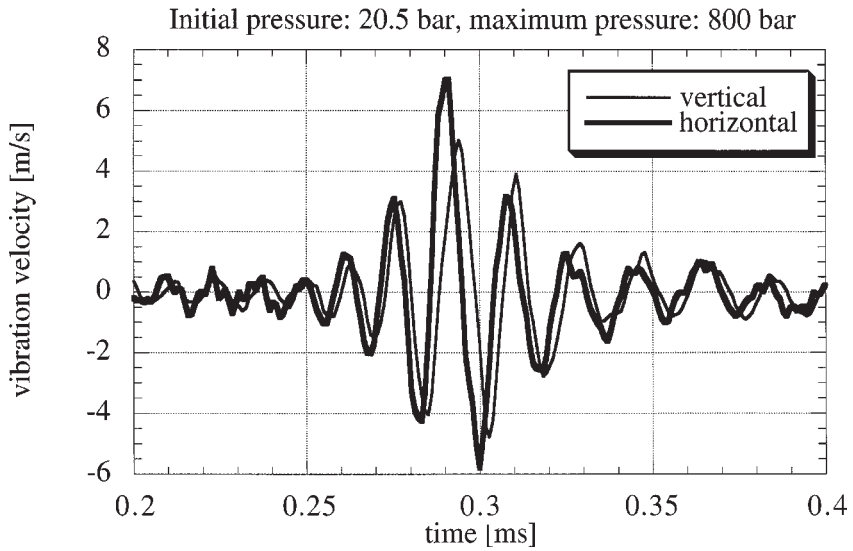

Fig. 7. Time series of radial vibration velocity.

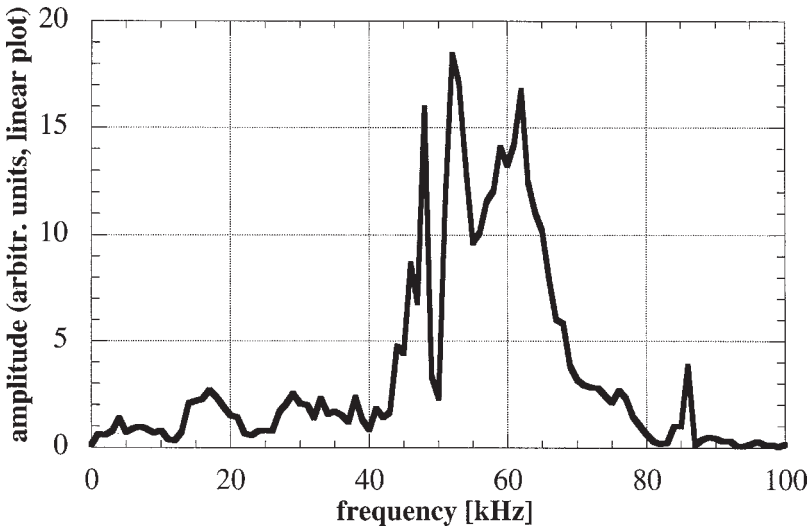

Fig. 8. Frequency spectrum of the radial vibration.

tion of the initial pressure. The data suggest that with increasing initial pressure the pressure ratio slightly decreases. But this effect was not examined any further.

4.3. Pipe wall vibrations

Figure 7 shows a typical time series of the measured radial vibration velocities of the pipe wall. The maximum values are of the order of 5–8 m/s, depending on the initial pressure.

The vibrations show a difference between the maximum radial vibration velocities in the horizontal and the vertical direction of up to 50%. There is no systematic trend between the two values to indicate which is the larger.

As in the case of the pressure, there is a typical value of the maximal value of around 1.1 m/s $\pm$25% for each 100 bar pressure peak. The displacement of the pipe wall reaches 5 μm peak-to-peak amplitude for each 100 bar pressure peak.

The frequency spectra of the radial vibration velocities (for example, Fig. 8) clearly indicate that differ-

ent vibration modes are excited by the detonation. That means that in reality the detonation front is not exactly symmetric because in this case only the rotational symmetric vibration mode would be excited. This is also shown by the trajectories in Fig. 9. Here, vertical velocities are plotted against horizontal velocities. The degree of asymmetry is clearly noticeable but dominating are the "nearly symmetric" modes.

Another interesting feature is a main frequency of around 55–60 kHz when the detonation front is just passing by. This can be seen in Fig. 10 where in the upper diagram a time series is shown. The time dependent FFT analysis in the lower diagram shows that this frequency is not present any more when the detonation wave has passed by. Then the symmetrical natural frequency of 45 kHz dominates.

Looking at the frequency spectra at a range of less than 2 kHz (see Fig. 11) there are clearly distinguished peaks which can be assigned to bending and axial vibration modes ($L_1, \ldots, L_4$). The axial modes are found via the lateral contraction obtained from the radial vibrations.

5. Radial vibration modelling (dynamic approach II)

In the following section, modelling approaches are given for the radial and axial vibrations of the pipe. They lead to general statements about the dynamical loading of pipes by detonations. The results of calculations and measured data are compared.

5.1. Calculation of the vibration mode with rotational symmetry in a pipe

The radial vibration mode with rotational symmetry in a pipe is calculated analytically under the following assumptions and approximations:

(1) The pipe wall is regarded as homogeneous.
(2) The pressure time history of the detonation is approximated by the exponential function $p(t) = p_\infty + (p_{\max} - p_\infty)\mathrm{e}^{-\alpha t}$, $p_\infty = p(t \to \infty)$. The damping factor α is approximated to $\alpha = 6000\text{–}7000\ \mathrm{s}^{-1}$ from the measurements. p_∞ is the final pressure. Caused by the high temperature of the reaction products, it is about 10 times the initial pressure: $p_\infty \approx 10 p_{\mathrm{ini}}$.
(3) The shock front associated with the detonation is not considered propagating through the pipe. It is assumed that the pressure is the same at any axial position in the pipe at a given time t.
(4) The pressure of the detonation at a time t is assumed equal at all points given by the intersection of a plane vertical to the axis of the pipe with the inner surface of the wall of the pipe (rotational symmetry). This means that of all possible radial vibration modes only the one with symmetry is excited.
(5) The circumferential stress generated in the pipe wall by the detonation is considered as uniform over the thickness of the wall (assumption of a thin walled tube).
(6) The pressure outside the pipe is neglected.

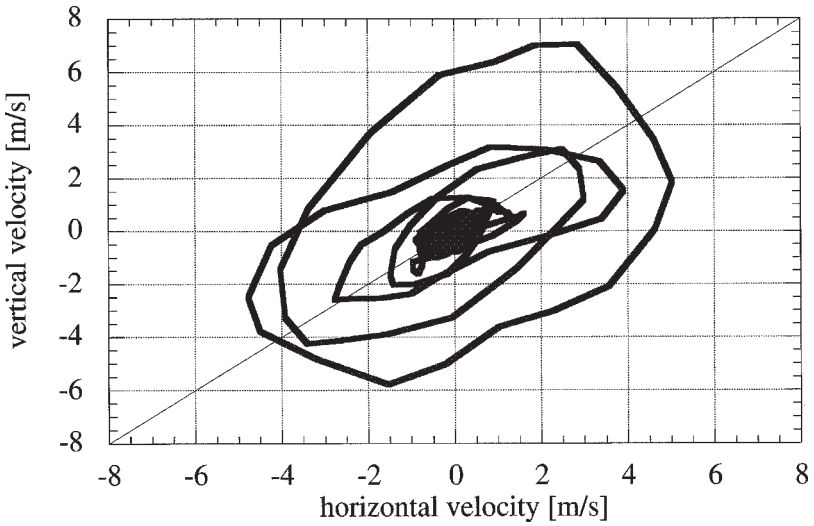

Fig. 9. Trajectories of the vertical/horizontal components.

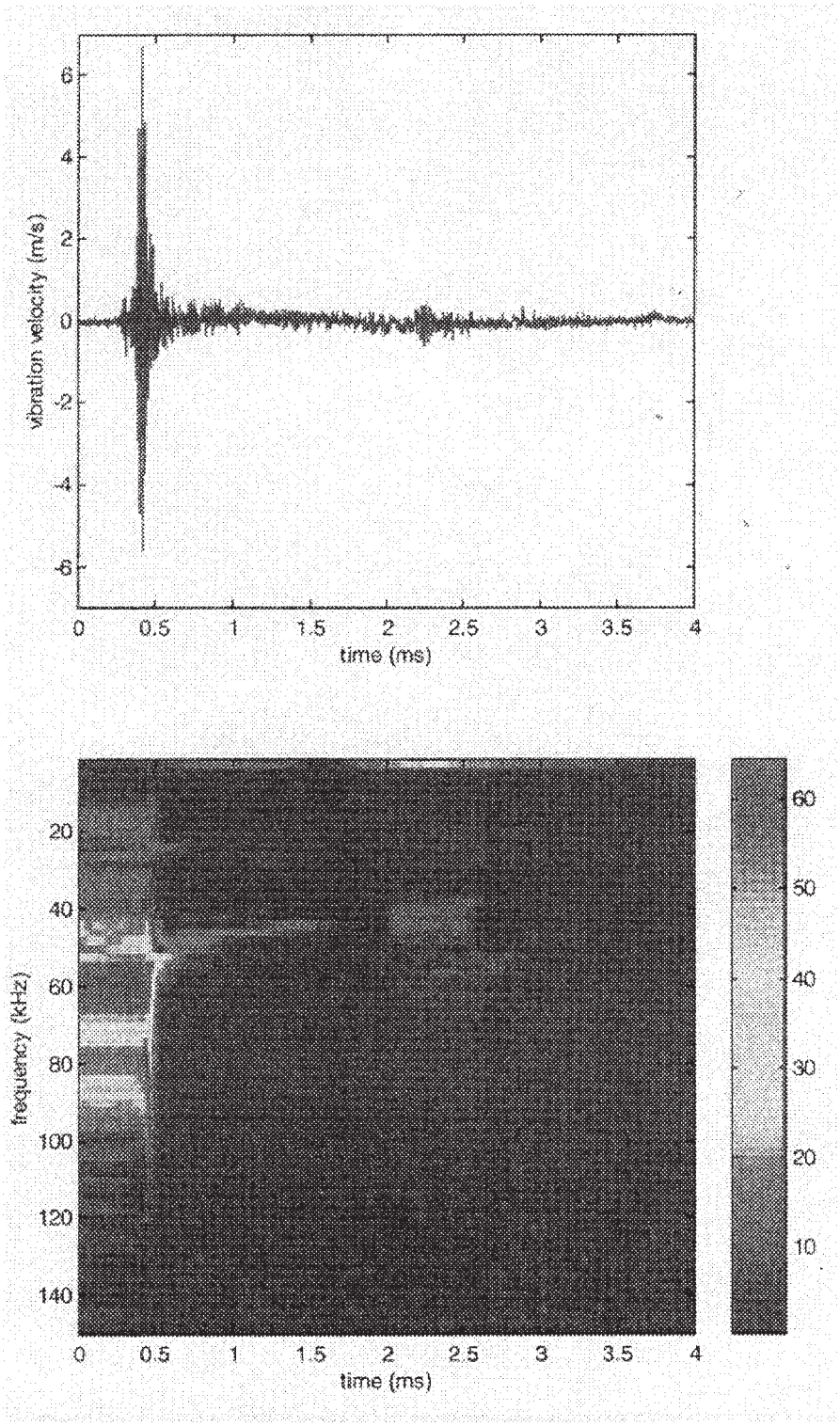

Fig. 10. Time dependent FFT analysis of a time signal.

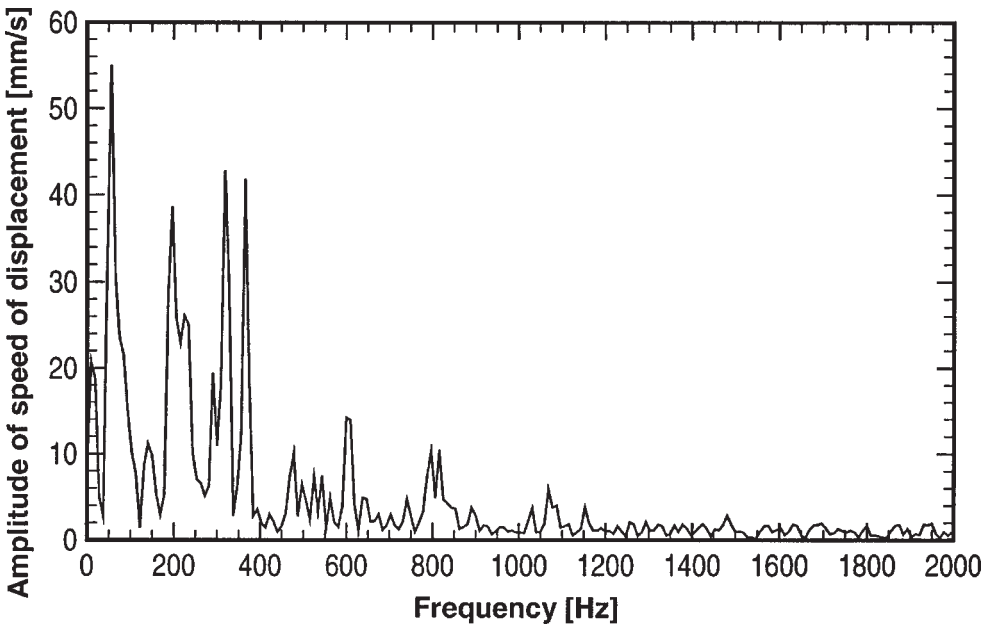

Fig. 11. Frequency spectrum in the low frequency range. Peaks can be associated with natural frequencies of bending and axial vibration.

(7) The wall material is regarded as totally elastic. No plastification effects are taken into account. This assumption holds as long as the stress caused in the wall of the pipe does not exceed the yield strength ($R_{p0.2}$) of the material.

The radial vibrations $u(t)$ are thus described by the damped one degree of freedom model

$$\ddot{u}(t) + 2\zeta\omega_R\dot{u}(t) + \omega_R^2 u(t) = Ap(t),$$
$$A = \frac{2\pi R_i}{\rho\pi(R_a^2 - R_i^2)}, \quad \omega_R = 2\pi f_R,$$

where the natural frequency of a thin walled tube is given by

$$f_R = \frac{1}{2\pi}\frac{c_L}{R} \quad \text{with} \quad \overline{R} = \frac{R_a + R_i}{2}.$$

The solution can be obtained analytically:

$$u(t) = \frac{Ap_0}{\omega_R^2}\left[1 - e^{-\zeta\omega_R t}\left(\cos\omega_R\sqrt{1-\zeta^2}t + \frac{\zeta}{\sqrt{1-\zeta^2}}\sin\omega_R\sqrt{1-\zeta^2}t\right)\right] + \frac{A(p_{max} - p_0)}{\alpha^2 - 2\zeta\alpha\omega_R + \omega_R^2}\left[e^{-\alpha t} - e^{-\zeta\omega_R t} \times \left(\cos\omega_R\sqrt{1-\zeta^2}t + \left(\frac{\zeta}{\sqrt{1-\zeta^2}} - \frac{\alpha}{\omega_R\sqrt{1-\zeta^2}}\right)\sin\omega_R\sqrt{1-\zeta^2}t\right)\right].$$

In case of homogeneous initial conditions, the approximated maximum amplitude is $u_{max} = Ap_{max}/\omega_R^2$. With the given geometry and material data we have $u_{max} = 1.63\,\mu\text{m}/100$ bar and $\dot{u}_{max} = 0.4$ m/s/100 bar. To illustrate the results, Fig. 12 displays the vibrations of a pipe excited by a pressure pulse due to a detonation.

To give some idea about the frequencies, maximum displacements and vibration velocities associated with the symmetric vibration mode, Table 1 displays the data for different tube geometries common for high pressure applications in process industry.

As in reality the pipe is not a thin walled cylinder, the calculated values are mean values. To obtain the maximum values which are found at the inner surface of the wall, as well as to compare to the measured values which are taken at the outer surface of the wall, the following relation has to be taken into account:

$$u(r) = \frac{(1+\nu)pR_i^2}{E(R_a^2 - R_i^2)}\left[\frac{R_a^2}{r} + (1-2\nu)r\right].$$

In the given case, the displacements at the inner surface will be 19% higher than the mean value. At the outer

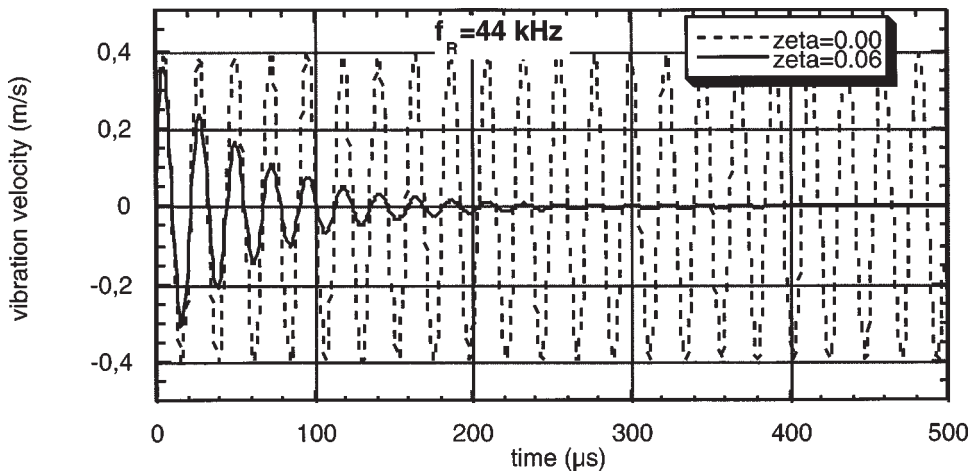

Fig. 12. Calculated displacements velocities excited by a pressure pulse due to a detonation. The equations allow for a vibration mode with rotational symmetry. Parameters: $E = 2.0 \times 10^{11}$ N/m^2, $\rho = 7900$ kg/m^3, $R_\mathrm{a} = 24$ mm, $R_\mathrm{i} = 15$ mm, $p_\mathrm{max} = 700$ bar, $f_\mathrm{R} = 44$ kHz.

Table 1

Frequencies, maximum displacements u_max (peak to peak) and vibration velocities $\dot{u}_\mathrm{max}$ (amplitude) for certain common tube geometries and different detonation pressures p_max. Calculation is based on a modulus of elasticity $E = 2.0 \times 10^{11}$ N/m^2 and a density $\rho = 7900$ kg/m^3. The wall material was assumed elastic

Radii of tube,	f_R (kHz)	T (μs)	$p_\mathrm{max} = 325$ bar		$p_\mathrm{max} = 1250$ bar	
R_i, R_a (mm)			u_max (μm)	$\dot{u}_\mathrm{max}$ (m/s)	u_max (μm)	$\dot{u}_\mathrm{max}$ (m/s)
$R_\mathrm{i} = 4$, $R_\mathrm{a} = 5$	178	5.6	5.7	3.2	22	12.3
$R_\mathrm{i} = 3$, $R_\mathrm{a} = 5$	200	5	1.9	1.2	7.3	4.6
$R_\mathrm{i} = 5$, $R_\mathrm{a} = 9$	114	8.7	2.7	1.0	10.7	3.8
$R_\mathrm{i} = 15$, $R_\mathrm{a} = 24$	44	24.3	10.3	1.3	39	5.1
$R_\mathrm{i} = 20$, $R_\mathrm{a} = 35$	29	34.3	11.6	1.0	45	4.1

surface, the displacements are 76% of those at the inner surface and 90% of those at the mean radius.

A finite element model which additionally considers the thickness of the pipe wall leads to a similar result. So, the radial displacements at the inner wall of the pipe and the wall stresses can be calculated from the measured radial displacements at the outer wall.

5.2. *Natural frequencies and modes of the radial vibrations of a pipe*

With a linear-elastic finite element model, all of the radial vibration modes and their natural frequencies can be calculated. Examples are given in Fig. 13. Some of the radial vibration modes may be as well calculated in terms of formulae. The rotational symmetric mode of the "thin walled tube" was already given with $f_\mathrm{R} = c_\mathrm{L}/2\pi\bar{r}$. Due to the wall thickness, the real frequency is somewhat smaller. As well, the "breathing" frequencies f_i can be calculated (see [1]) by

$$f_i = \frac{1}{2\pi}\frac{i(i^2-1)}{2\sqrt{3}\sqrt{i^2+1}}\frac{c_\mathrm{L}}{\overline{R}}\frac{(R_\mathrm{a}-R_\mathrm{i})}{\overline{R}},$$
$$i = 2, 3, \ldots .$$

Some of these vibration modes appear as well in the measured frequency spectra. Mainly, there are modes with the frequencies of 14, 38, 45, 60 and 88 kHz as already shown in Fig. 8. A frequency at around 50–60 kHz is not present.

5.3. *Effects of asymmetric excitation*

With finite element calculations, the effects of asymmetric excitation are studied. Different load cases with the same time history are studied. Three cases are compared here:

Case 1: symmetrical loading;
Case 2: load only acting on 270° of the pipe;
Case 3: point load at one point.

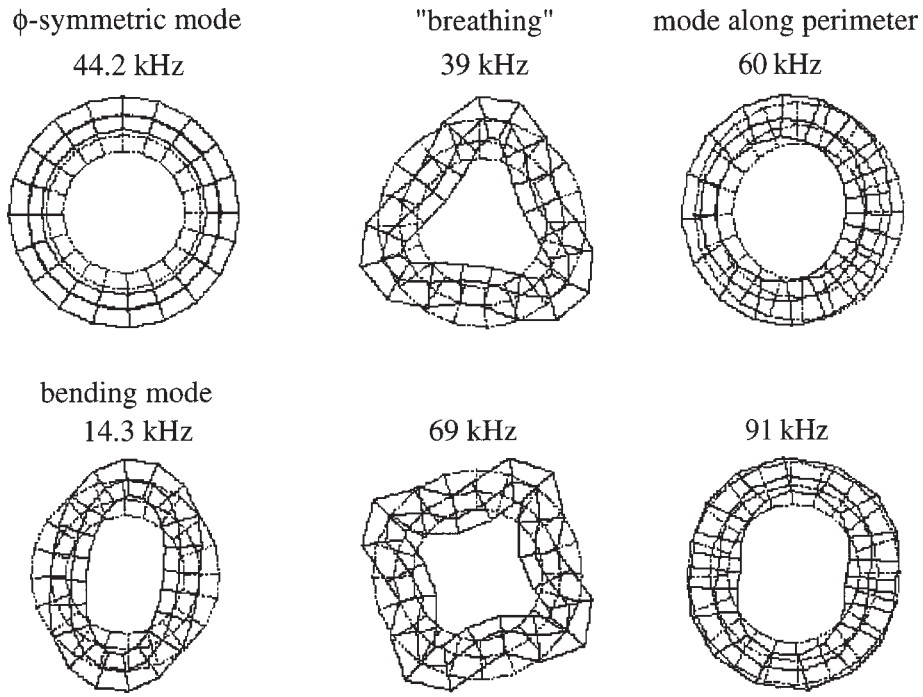

Fig. 13. Natural frequencies and modes of the radial vibrations of a pipe, calculated by a linear-elastic FE model.

	Simulation	Measurement	Measured/ Simulated
Maximum displacement (μm)	2.57	4.8–6.3	1.8–2.4
Maximum velocity (m/s)	0.36	0.9–1.2	2.5–3.3
Maximum acceleration (m/s^2)	98300	250000	2.5

The main result is the following: with increasing asymmetry it is possible that locally the vibration amplitudes as well as the stresses are much higher than in the symmetric case (factors up to 10).

6. Comparison between measurements and simulation

The following table shows a comparison between measured and calculated data. The calculated data are corrected for the outer pipe wall and related to a pressure peak of 100 bar.

The results of the different experiments are shown in Fig. 14. The tangential stresses are shown in Fig. 15. The theoretical values obtained by approach II are substantially smaller than the measured values. Thus, there is a Dynamic load factor (DLF) of about 2 to 3 which is not included in the simple model. Three effects are influencing this DLF:

- Thick-walled pipe. Difference between values at mean radius and maximum values at inner pipe wall, as mentioned above.
- Non-symmetric behaviour resulting from loading and geometry as mentioned above.
- Wave propagation effects.

6.1. Comments on wave propagation effects

Pfefferkorn [4] investigated theoretically the radial displacements of a pipeline due to a travelling pressure rise. The investigation was initiated by the rupture of a PVC pipe where the rupture moved over the whole pipe length with sonic speed. For his investigations he used wave propagation theory. The main difference is in the load history. For the PVC pipe a sudden pressure jump was modelled, whereas here we have a short time pressure pulse. Qualitatively and quantitatively, some of the results are transferable.

After “starting up” the pressure front and without considering reflections at the pipe end, there is a typical wave form which steadily moves along the pipe with the propagating speed of the detonation front. The

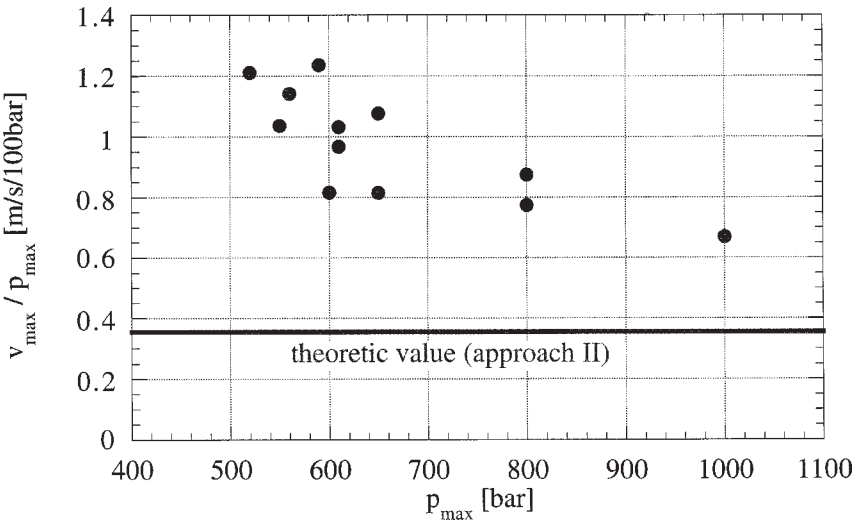

Fig. 14. Comparison between measured and theoretical values of the vibration velocities. The vibration velocities obtained in different experiments at different initial acetylene pressures were scaled by dividing through the respective detonation pressure $p_{\max}$, which was expressed in multiples of 100 bar.

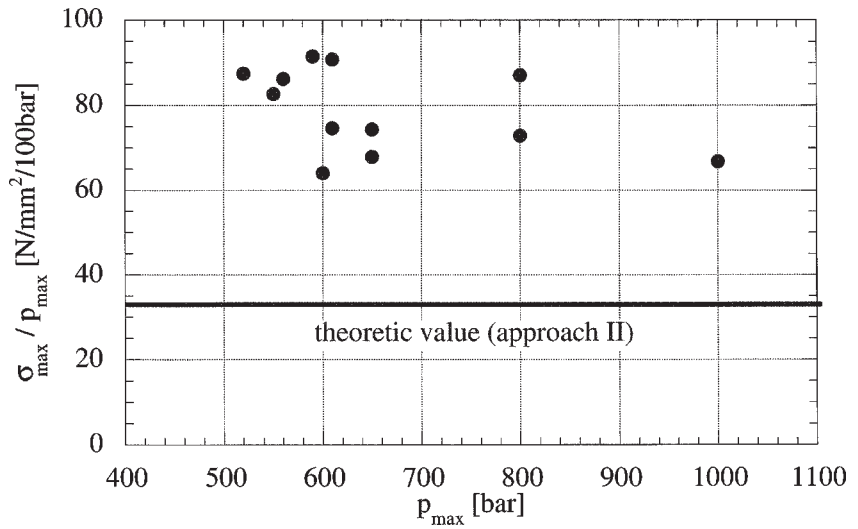

Fig. 15. Comparison between measured and theoretical values of the tangential stresses. The tangential stresses obtained in different experiments at different initial acetylene pressures were scaled by dividing through the respective detonation pressure $p_{\max}$, which was expressed in multiples of 100 bar.

wave form itself depends on the Mach number of the moving detonation front as function of the propagation velocity of the transverse wave c_{T} and the pipe geometry. Typical steady wave forms are represented in Fig. 16. The amplitude overshoots are significant. When the Mach number reaches 1 there are resonance effects.

The amplitudes are not directly transferable to the actual load case; but the wave length is. For the case $\mathrm{Ma} = 0.73$ there is a wave length of $X = 0.05$ m. The corresponding frequency of the travelling wave is $f_{\mathrm{W}} = c_{\mathrm{T}}/X = 58$ kHz. This corresponds very well with the measured main frequency at the point in time at which the detonation front passes by.

This also explains why the pipe wall is deformed "slowly" as it can be seen in Fig. 7, i.e., with two periods of increasing amplitudes already before the detonation front passes by.

Thus, the wave propagation effects seem essentially for a more exact calculation of vibration amplitudes

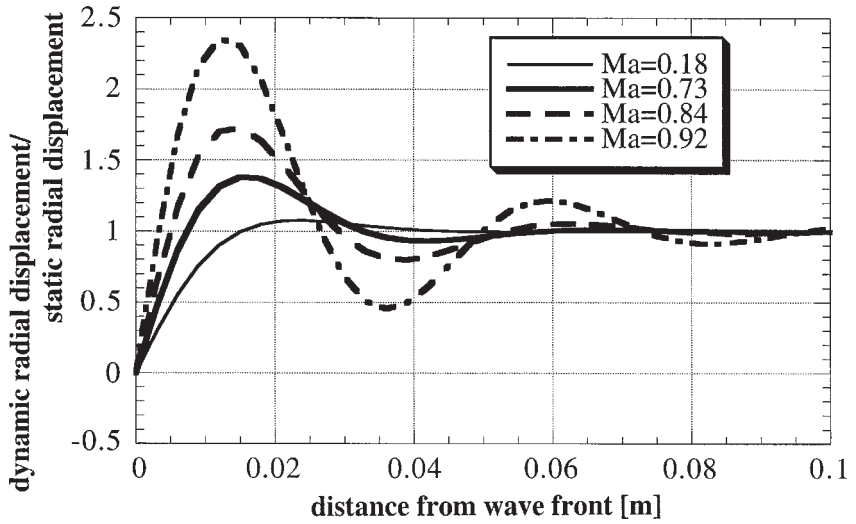

Fig. 16. Wave forms for different propagation speeds of the detonation front, calculated for the tube with inner radius $R_{\mathrm{i}} = 15$ mm and outer radius $R_{\mathrm{a}} = 24$ mm.

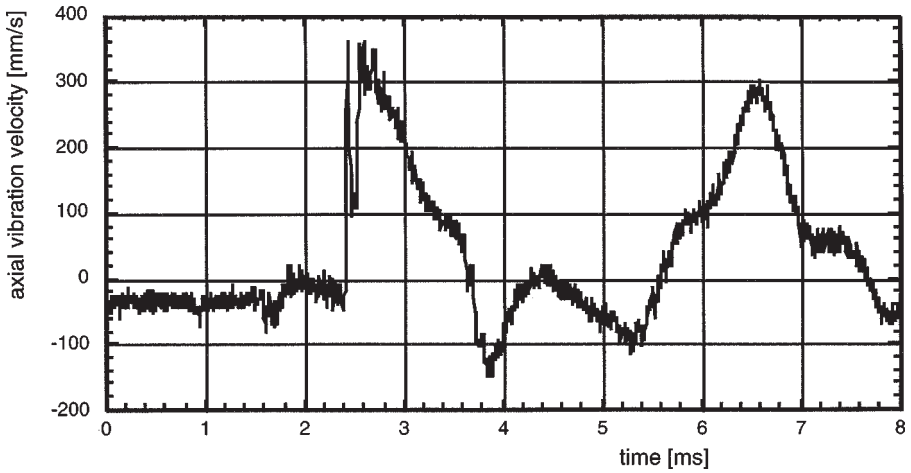

Fig. 17. Time signal of the axial vibrations at the blind flange (position 4 in Fig. 3, laser vibrometer measurements).

and the tangential stress and have to be examined further.

7. Comments on the longitudinal vibrations

Another aspect which can be perceived by the measurements is that of the axial vibrations of the pipe which are excited by the reflexion of the detonation wave at the closed end. The axial displacements are obtained from the radial displacements via the Poisson number and compared to the direct laser vibrometer measurements at the blind flange (pos. 4 in Fig. 3). They can be distinguished due to the much lower frequency range of axial vibrations.

With the assumption of the boundary conditions "fixed end at ignition side, free end at blind flange" we calculated the natural frequencies as

$$f_{i,ax} = \frac{1}{2\pi}\beta_{i,ax}\frac{c_{\mathrm{L}}}{L}, \qquad \beta_{i,ax} = \left(i - \frac{1}{2}\right)\pi, \qquad i = 1, 2, \ldots,$$

with the values 210, 630, 1050, 1480 Hz very close to those which were measured (see Fig. 11).

The calculation of the corresponding axial vibration amplitudes is achieved with a Timoshenko beam model

for position 3. The pressure excitation of the pipe end is $F(t) = 2p(t)\pi R_i^2$. E.g., for a maximum pressure of 620 bar the axial vibration velocity at position 3 will be 278 mm/s.

The measured maximum of the *radial* velocity which corresponds to the *axial* vibration frequencies can be estimated from the time signal. The conversion leads to results within an accuracy of $\pm 20\%$.

The time signal of the direct measurement of the axial vibrations at position 4 is shown in Fig. 17. Converted to position 3, it also leads to the result of 290 mm/s.

8. Summary

The dynamic response of a pipe wall on a detonation was investigated by measurements using laser velocimetry and by theoretical considerations. There was good agreement between measured and predicted values of vibration frequencies, but discrepancies in the radial displacements and vibration velocities which were mainly due to wave propagation effects. There is a dynamic load factor of around 2 to 3 which is not included by model approach II. It was found that various radial vibration modes other than the fundamental one (rotational symmetry) are excited. This may be attributed to the complex structure of the detonation front which is not just a plane of high pressure oriented vertical to the axis of the pipe.

The propagation velocities of longitudinal and transverse waves and the detonation front can also be detected. Wave propagation was shown to have a strong influence on the results. Its effects have to be studied further to be able to quantify better the dynamic load on the pipe and its consequences on tangential stress. This is currently under investigation and the results will be published elsewhere.

In this paper, no focus has been given to the stresses in the wall of the pipe. They can be calculated from the radial displacements of the wall or the model approach II including the dynamic load factor. It can be shown that if the load of the wall is applied by a detonative pressure pulse the wall can withstand higher stresses than in case of applying the load as a static pressure. This is because the yield strength of the material is increased by factors up to 2 because of the high strain rates resulting from detonative application of the load (strain rates are of the order of $10^6\ s^{-1}$). Details on this aspect are published in [6].

References

[1] J.P. den Hartog and G. Mesmer, *Mechanische Schwingungen*, Springer Verlag, Berlin, 1952, p. 191.

[2] D. Lietze, Anlaufen von Detonationen im Inneren geschlossener Systeme, *Erdöl und Kohle* **46** (6) (1993), 251–257.

[3] D. Lietze, Beanspruchung von Rohrleitungen bei detonativ verlaufenden Gasreaktionen, *TÜ* **36** (6) (1995), 264–267.

[4] W. Pfefferkorn, Die Beanspruchung der Rohrwand durch eine wandernde Druckstörung, *Chem. Techn.* **32** (4) (1980), 189–192.

[5] M.W. Ringer, Detonation tests and response analyses of vessels and piping containig gas and aerated liquid, *Plant Oper. Prog.* **4** (1) (1985), 26–47.

[6] H.P. Schildberg, A. Sperber and M. Walter, Quantification of the load acting on the wall of pipes when exposed to detonations, in: *1st Internet Conf. Process Safety*, 1998, http:// www. prosicht. com/conference.

[7] M. Sichel, C.W. Kauffman and Y.C. Li, Transition from deflagration to detonation in layered dust explosions, *Process Safety Progress* **14** (1995), 257–265.

[8] N.N. Smirnov and I.I. Panfilov, Deflagration to detonation transition in combustible gas mixtures, *Combustion and Flame* **101** (1995), 91–100.